OTEKON 2012
6. Otomotiv Teknolojileri Kongresi
04 – 05 Haziran 2012, BURSA

COMPARISON OF CONSTITUTIVE HYPER-ELASTIC MATERIAL MODELS IN FINITE ELEMENT THEORY

Savaş Kayacı, Ali Kamil Serbest
Las-Par Rubber Components and Development Ltd. Co.
Akcalar Industrial Zone Kale Street No.10 16225 Nilufer Bursa/Turkey

ABSTRACT

This study aims to investigate the most widely used hyper-elastic material models applied in finite element solutions of large deformation problems. Physical tests were carried out on specimens which are loaded under compression, simple shear and tension to obtain the stress-strain data for all loading modes, respectively. For the same physical tests, finite element models were constructed. Mooney-Rivlin material model with 2 and 3 constants and Ogden model with 2 and 3 coefficients, derived from the stress-strain data under compression, shear and tension. Resulted material models are implemented in finite element solutions of the physical tests. The results of finite element solutions were discussed and compared with the real test results. They are also compared to each other to see which models are more accurate. At the end, a finite element analysis is performed for a real life example; an Anti-vibration mount. The results of quasi-static experiment of an anti-vibration mount and corresponding finite element analysis were also discussed and compared.

Keywords: Finite element theory, hyper-elastic material models, mechanical properties of rubber.

1. INTRODUCTION

Today, rubber is one of the most important engineering materials that an engineer can use to solve a particular problem in every field of industry. One can use rubber as an engineering raw material in many fields like defense, automotive, ship building, machinery, aviation, etc. The main uses of rubber in these industries are;

- Sealing,
- Vibration and shock isolation,
- Liquid transportation.

Because of its ability to withstand very large deformations and its energy absorption properties, engineers very often use parts made of rubber in vibration and shock isolation problems. In some applications rubber is selected as the raw material of a sealing element because of its resistance against high pressure, high temperature and different degraders. The same reason also makes rubber as a unique material for liquid transportation systems like hoses and custom-shape pipes.

Rubber can be classified as an isotropic raw material but its mechanical properties cannot be expressed by linear expressions like Hooke's Law. Since there is no linear relationship between stress and strain values when a rubber block is subjected to a certain deformation, a different approach should be developed to define the relationship between stress and strain values of a hyper-elastic material. The reason, why a simple relation cannot be used, is that rubber is considered to be an incompressible material (e.g. poissons' ratio is equal to 0.5). Considering a cubic element of unit dimension, one can express the bulk modulus as follows.

$$K = \frac{E}{3(1-2\nu)} \qquad [1]$$

Where, K: Bulk modulus,
E: Modulus of elasticity,
ν: Poissons' ratio.

If one plugs the poissons' ratio as 0.5 into Equation 1, the bulk modulus value becomes infinity. This reason makes it impossible to obtain a simple mathematical

model to characterize the mechanical properties of rubber or rubber like materials in finite element theory, accurately.

In the past, many studies were carried out obtaining a good constitutive mathematical model to express the mechanical properties of rubber. In some studies rubber is assumed to be compressible materials while in some other studies it is assumed to be fully incompressible material. Many authors have derived expressions using the strain energy theory. The constitutive material models for hyper-elasticity can be classified into two different groups; in one group the strain energy density function is assumed to be a polynomial function of three principal strain values, in the other group it is a separable function of three principal strain values.

Peng et al presented finite element formulations based on a compressible strain energy function[1]. They modified Ogden-Tschoegl model by adding a shear term and derived the bulk term from an experimental relationship between hydrostatic pressure and volume ratio. They also proposed that penalty method can be used to modify an incompressible strain energy function to a compressible one. This study concluded that either the compressible approach or the penalty method is a robust analysis procedure for hyper-elastic materials.

Arruda and Boyce proposed a constitutive model based on an eight chain representation of the underlying macromolecular network structure of the rubber and non-Gausian behavior of the individual chains in the proposed network[2]. They concluded that eight chain model predicts the mechanical behavior of materials accurately after comparing the experimental and numerical results they obtained.

Sasso et. al. performed an experimental study to get the stress-strain behavior of an hyper-elastic material and use the data to determine the coefficients of hyperelastic material models[3]. In this paper, the experiments are also simulated by using the obtained material models. They concluded that the results of FEM solutions gave a useful comparison with the real test results.

Selvaduari made a study on deflections of a rubber membrane after retrieving material model coefficients for several hyper-elastic material models from dumbbell specimen loaded in uni-axial tension[4]. In his study it is concluded that the best correlation between the numerical results and real results can be obtained by simpler strain energy functions like used in Mooney-Rivlin or Baltz-Ko material models.

Kim et. al. studied the nonlinear properties of polydimethylsiloxane(PDMS)[5]. They carried out a uniaxial tensile test by using thin strip specimens They also examined the effect of different formulations of PDMS compounds on the final mechanical properties. The conclusion of this study is that a second order Ogden material model more properly describes the material model than Neo-Hookean and Mooney-Rivlin material models.

Gent also discussed and compared the hyper-elastic material models based on their accuracies with the real test data [6]. He ended up such conclusions: A Neo-Hookean, Mooney-Rivlin material model gives good correlation with a uniaxial tensile test data up to 40% strain and with a simple shear data up to 90% strain and it exhibits a constant shear modulus. A two coefficients Mooney-Rivlin material model can give good agreement up to 100% strain for a tensile loading, while it is inadequate of describing compressive behaviors when a specimen is loaded under compression. It also can not show the stiffening of material at large strain values. Higher order Mooney-Rivlin models can account for a non-constant shear modulus but they should be used with caution since higher order terms may make the strain energy function unstable outside the range of experimental data. This would result in unrealistic mechanical behaviors. The Ogden material model also takes a non-constant shear modulus into account and can give accurate results up to 700% strain in simple tension. However it can show a slightly compressible behavior.

The mathematical description of material models is out of the scope of present study. However, it is better to explain how to find the material coefficients using the experimental stress strain data. For this purpose, a procedure to find the coefficients of Mooney-Rivlin material model for a simple tension data is given in the followings [6].

$$\lambda = \frac{L_f}{L_o} \qquad [2]$$

$$\sigma = \frac{F}{A} \qquad [3]$$

Where, λ: deformation state,
L_f: length of the spec. at any deformation,
L_o: original length of the specimen,
σ: Engineering stress,
F: Load at any deformation,
A: Non-deformed cross sectional area.

Using the terms in Eqn.2 and Eqn.3, one can write the stress-strain equation for Mooney-Rivlin material model as follows[6]:

$$\sigma = 2(\lambda - \lambda^{-2})(C_1 + C_2(\lambda^{-1})) \qquad [4]$$

Where, C_1 and C_2: are coefficients. This equation can be plotted as $\sigma[2(\lambda-\lambda^{-2})]$ against $1/\lambda$. On this graph, the intercept at $1/\lambda=1$ gives the value of C_1+C_2. The value of C_2 can be obtained from the positive slope of straight section of curve.

The coefficients can be calculated by using the strain energy functions for any hyper-elastic material model. However, it is recommended to use the subroutines included in the commercial FEM software.

In the present study, only 2nd and 3rd order Mooney-Rivlin and Ogden hyper-elastic material models are used and their accuracies are discussed for natural rubber compounds of different hardness under simple shear, simple tension and compression.

2. EXPERIMENTS

Mechanical behavior of rubber should be considered and determined separately for tension, shear and compression. Therefore, the following test specimens are used to get the stress-strain properties for tension, compression and shear, respectively.

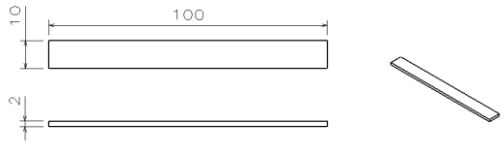

Figure 1. Tension specimen.

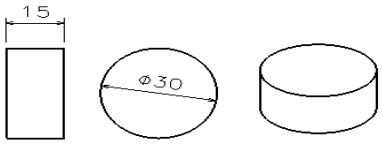

Figure 2. Compression specimen.

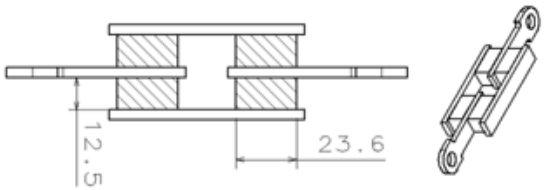

Figure 3. Simple shear specimen (width=12.5 mm).

Tensile Test:

Tensile tests were conducted on "Shmiadzu AG-I 10" test machine, which has a load cell capacity of ±10kN, according to the test parameters given below.

Table 1. Tension test parameters.

Temperature (°C)	RT
Pre-load (N):	5
# of pre-conditioning cycles:	3
Pre-conditioning speed (mm/min):	200
Pre-conditioning load (mm):	150
Test speed (mm/min):	20
Test load (mm):	150

The preparation of tensile test specimens is very important. They should be marked by a white color pen to let the video extensometer to record the elongation between the markings. The markings are distanced 50 mm away from each other. During the test, specimens are preloaded by 5N in tension to ensure that they are in tension. Then they are elongated 3 times at a speed of 200 mm/min till 150 mm to eliminate the Mullin's effect. After the preconditioning cycles, in the 4th cycle load displacement data are collected.

Compressive Test:

For compression disks, the friction on bottom and upper surfaces is important and should be eliminated to get the test data properly. Therefore, these surfaces are lubricated with a non-aggressive lubricant just before the test. The specimens are not to be fully submerged and kept in lubricant since it may change the properties of rubber.

Compressive tests are performed on "MTS 831.10 Elastomer Test Machine". This machine is a hydraulic test machine equipped with a load cell of ±25kN and a piston of maximum 60 mm stroke. It can also bear with a frequency of maximum 200 Hz.

The tests are carried out according to the parameters given in Table 2. Pre-conditioning cycles are again necessary to eliminate Mullin's effect.

Table 2. Compression test parameters.

Temperature (°C)	RT
Pre-load (N):	-10
# of pre-conditioning cycles:	3
Pre-conditioning speed (mm/min):	100
Pre-conditioning load (mm):	-7.5
Test speed (mm/min):	10
Test load (mm):	-7.5

Shear Test

Shear tests are also performed on "MTS 831.10 Elastomer Test Machine". The specimens are fixed from both ends and elongated apart. This displacement creates a shear loading for each rubber pad bonded to rigid substrates. The tests are carried out according to the parameters given in Table 3.

Table 3. Shear test parameters.

Temperature (°C)	RT
Pre-load (N):	-10
	3
Pre-conditioning speed (mm/min):	100
Pre-conditioning load (mm):	-7.5
Test speed (mm/min):	10
Test load (mm):	-7.5

The specimen geometry for shear tests is selected to be a quad-pad specimen because it eliminates the bending moment which is expected at higher shear strain values.

3. RESULTS & CALCULATIONS

The load displacement values should be first converted to engineering stress-strain values to let the FEM software to calculate the material coefficients for different hyper-elastic material models. One can use the following formulas to calculate the engineering stress and strain, respectively.

$$\sigma = \frac{F}{A} \quad [5]$$

$$\varepsilon = \frac{L_i - L_o}{L_o} \quad [6]$$

Where, σ: engineering stress,
ε: engineering strain,
F: load,
A: un-loaded cross-section,
L_i: length at any deformation,
L_o: original length,

Above equations can only be applied to the results of compression and tension tests.In order to find the shear stress and strain values, the following equations are used.

$$\tau = \frac{F}{A} \quad [7]$$

$$\gamma = \frac{d}{t} \quad [8]$$

Where, τ: shear stress,
γ: shear strain,
F: load,
A: Cross-section area parallel to load,
d: shear displacement,
t: original thickness,

Stress strain diagrams for each compound are given in the next section "Finite Element Solutions". They are also compared with the results obtained from finite element analyses. Force displacement values can be used to calculate the hysteresis of compounds. Hysteresis can be calculated using the following formula:

$$HYS = \frac{E_{recovered}}{E_{in}} \quad [9]$$

Where, HYS is the designation of Hysteresis, E_{in} *(Nmm)* is the amount of energy applied to the rubber specimen during loading and $E_{recovered}$ *(Nmm)* is the amount of energy recovered during unloading. The difference, which is called E_{loss} *(Nmm)*, between these two energy values is absorbed by rubber specimen. The change in HYS depending on rubber hardness is given in Figure 4 for shear and compression loading modes.

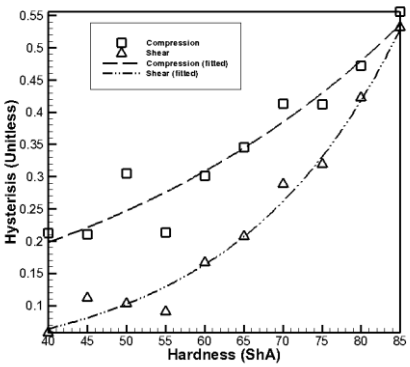

Figure 4. Hysteresis vs. hardness graph.

Modulii of elasticity in compression, shear and tension for hyper-elastic materials can be calculated at relatively lower strain values because of the fact that mechanical behavior of hyper-elastic materials are not linear. Only a portion up to a strain limit can be considered as linear and according to this portion of curve an average slope is calculated as the modulii of elasticity. In this study, modulus of elasticity of compounds is calculated up to a strain limit of 0.3. The following figure shows how modulii of elasticity changes depending on hardness for three principal loading modes.

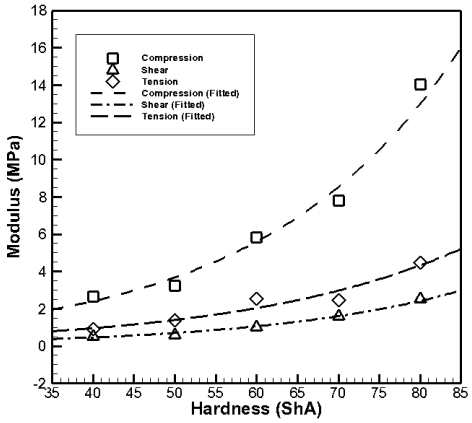

Figure 5. Modulus of elasticity vs. hardness graph.

One can find empirical relations regarding the relations between HYS and hardness also between elasticity and hardness. The most suitable curve fit function for these relations is an exponential function of the following form.

$$HYS = e^{AH+B} \quad [10]$$

$$E = e^{CH+D} \quad [11]$$

Where, E is called modulus of elasticity, H is called hardness of compound and A, B, C and D are curve fit coefficients. The coefficients are listed in the Table 4.

Table 4. Coefficients of curve fit functions.

Loading mode	Coefficient	Value
Compression	A	$2.215x10^{-2}$
	B	-2.506
Shear	A	$4.699x10^{-2}$
	B	-4.631
Compression	C	$4.213x10^{-2}$
	D	$-8.07x10^{-1}$
Shear	C	$4.13x10^{-2}$
	D	-2.422
Tension	C	$3.757x10^{-2}$
	D	-1.544

The values given in Table 4 are only valid for the intended compounds Las-Par Ltd. Co. produces. Therefore, the use of these empirical relations for compounds of other producers may lead the engineers to failure in the design of robust parts.

4. FINITE ELEMENT SOLUTIONS

The finite element calculations are performed using MSC Marc 2008 solver. Pre and post processing are done in MSC Patran 2008. For each specimen type, 8 noded hexahedral elements with an average global edge size of 2mm are used to construct the finite element models. The problems are assumed to be static problems, therefore static FEM analyses were run. Detailed boundary conditions are given in the following figures for each type of analyses.

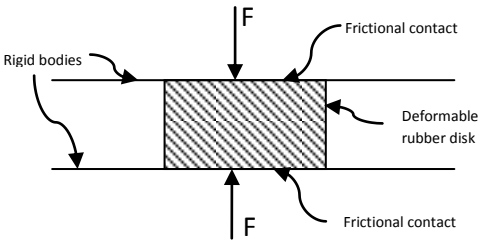

Figure 6. Boundary conditions of compression analysis.

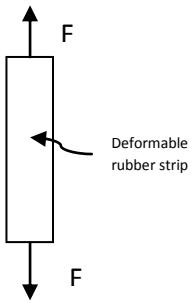

Figue 7. Boundary conditions of tension analysis, width is 2mm.

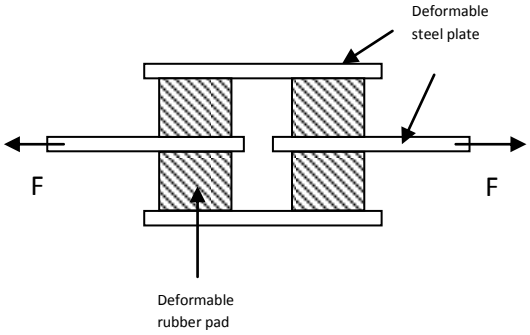

Figure 8. Boundary conditions of shear analysis.

Formulation of hyper-elastic elements was defined to be a Herrmann Reduced Integration formulation. For steel elements, the formulation is defined to be reduced integration.

In the case of compression analysis, the friction model was selected to be Coulomb for Rolling with a friction coefficient of 0,01. The friction coefficient was selected so low because the contact surfaces were fully lubricated by oil. For the steel plates, the material property data was obtained from a previous study made by Serbest and Kayacı [7]. In their study, They used a piecewise linear function to define plastic properties of a steel alloy with a very good agreement to the experimental results they obtained.

In the construction of FEM model for tensile specimen, a non-uniform mesh distribution is applied to compensate high level of distortion at high tensile strains. The height of the elements at the mid section kept as low as possible and increased gradually as the position of elements get closer to the ends of tensile specimen.

The following Figures 9 to 23 show the precision and accuracy of Mooney Rivlin and Ogden material models with respect to the real test results. Also a tabular representation of this comparison at lower strain values is given in Table 5.

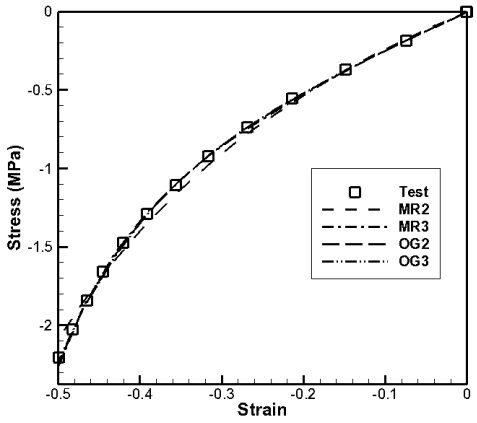

Figure 9. Compressive stress-strain relation of NR40 compound

Because of the quality of test data, complete range of the measurements could not be used to calculate the material model coefficients thus the strain range of the real test data was narrowed accordingly.

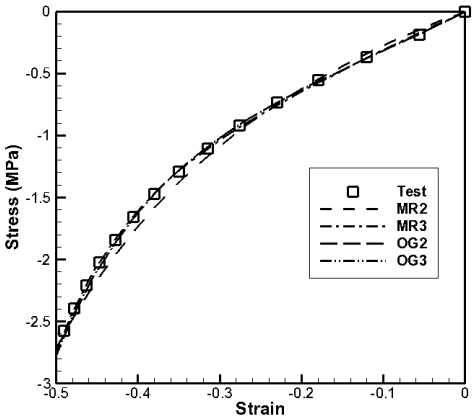

Figure 10. Compressive stress-strain relation of NR50 compound

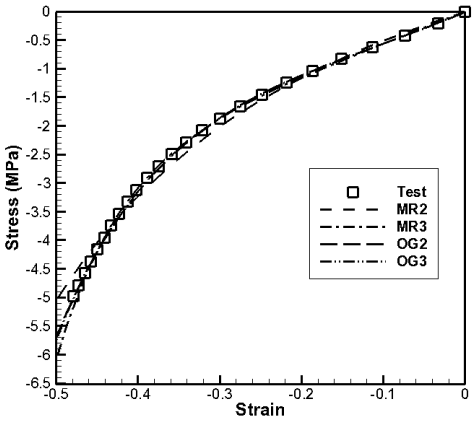

Figure 11. Compressive stress-strain relation of NR60 compound

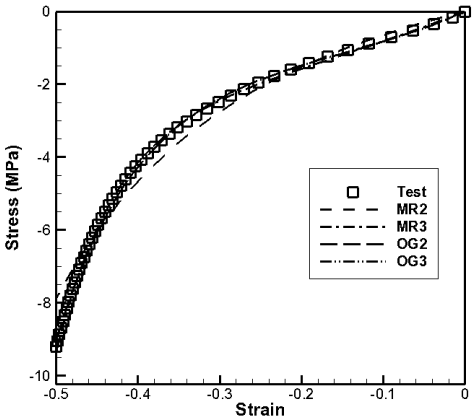

Figure 12. Compressive stress-strain relation of NR70 compound

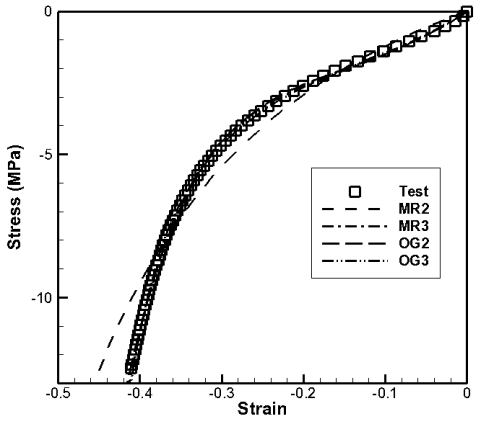

Figure 13. Compressive stress-strain relation of NR80 compound

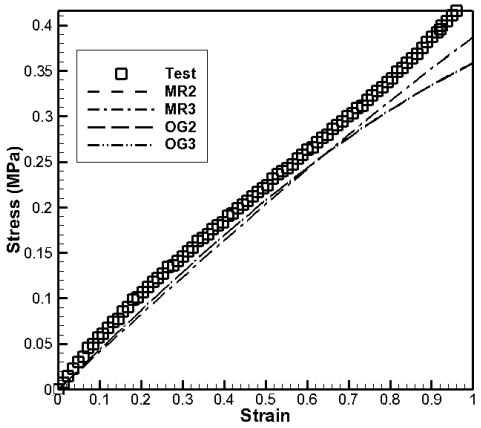

Figure 14. Shear stress-strain relation of NR40 compound

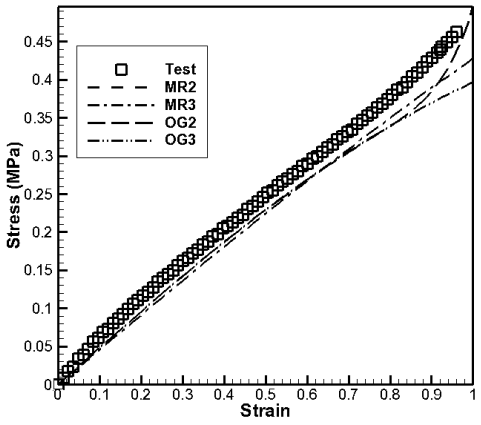

Figure 15. Shear stress-strain relation of NR50 compound

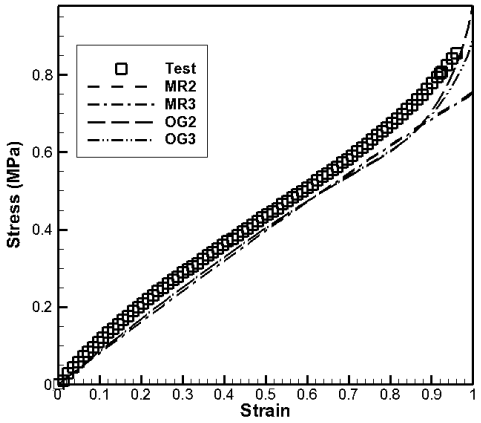

Figure 16. Shear stress-strain relation of NR60 compound

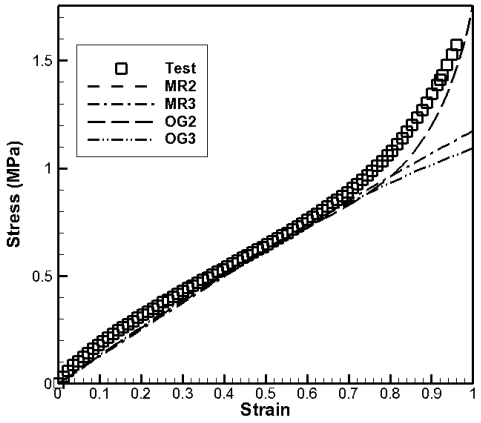

Figure 17. Shear stress-strain relation of NR70 compound

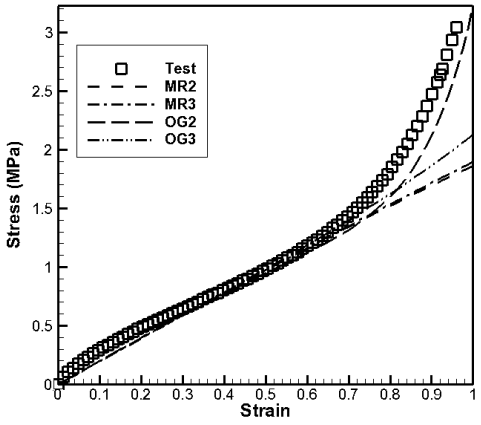

Figure 18. Shear stress-strain relation of NR80 compound

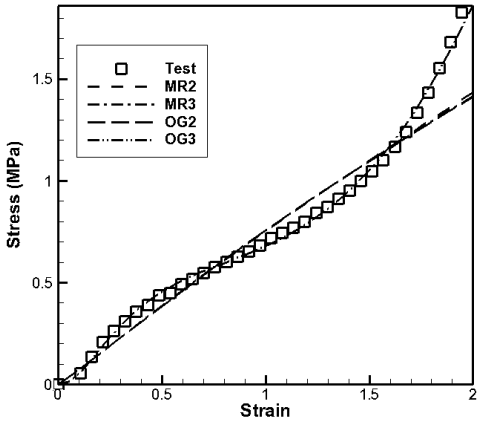

Figure 19. Tensile stress-strain relation of NR40 compound

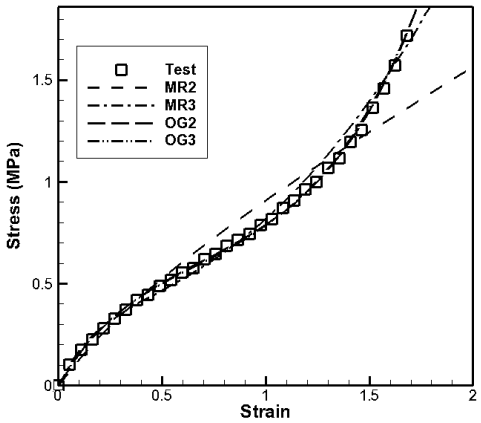

Figure 20. Tensile stress-strain relation of NR50 compound

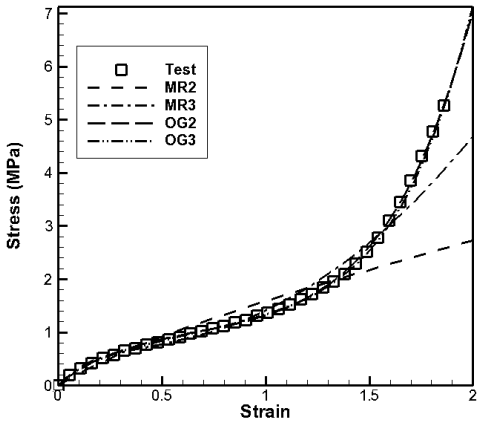

Figure 21. Tensile stress-strain relation of NR60 compound

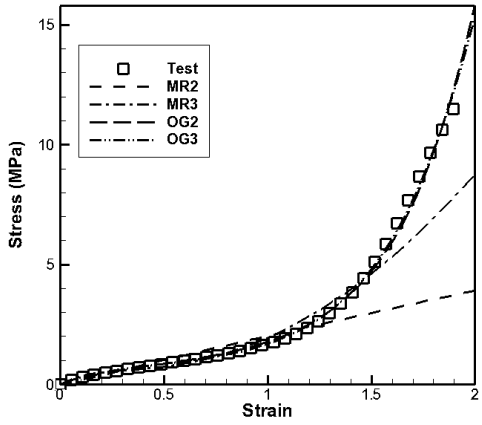

Figure 22. Tensile stress-strain relation of NR70 compound

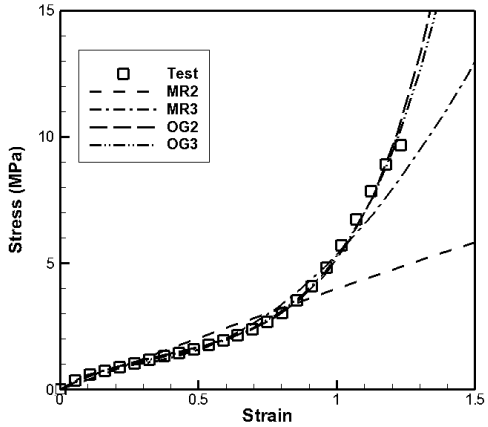

Figure 23. Tensile stress-strain relation of NR80 compound

Individual stress-strain comparison graphs for each hardness were given to see the accuracies of each material models for different natural rubber compounds of different hardness.

The stress-strain curves for the hyper-elastic material models were obtained by using the force-displacement data taken form finite element analyses runs for each principle loading mode and compound. In other words, equations 5, 6, 7 and 8 can be used to calculate the stress-strain data for each hyper-elastic model of different number of coefficients.

Table 5. Comparison at lower strain values

Mode	Strain	Engineering Stress (Mpa)	Computed Stress (Mpa)							
			MR2	Error (%)	MR3	Error (%)	OG2	Error (%)	OG3	Error (%)
Compression	NR40									
	-0.1	-0.251	-0.243	-3.19	-0.253	0.80	-0.252	0.40	-0.251	0.00
	-0.2	-0.516	-0.537	4.07	-0.53	2.71	-0.524	1.55	-0.52	0.78
	-0.3	-0.86	-0.909	5.70	-0.861	0.12	-0.856	-0.47	-0.856	-0.47
				2.19		1.21		0.49		0.10
	NR50									
	-0.1	-0.311	-0.279	-10.29	-0.313	0.64	-0.319	2.57	-0.318	2.25
	-0.2	-0.628	-0.628	0.00	-0.648	3.18	-0.634	0.96	-0.633	0.80
	-0.3	-1.035	-1.089	5.22	-1.042	0.68	-1.02	-1.45	-1.022	-1.26
				-1.69		1.50		0.69		0.60
	NR60									
	-0.1	-0.555	-0.518	-6.67	-0.571	2.88	-0.573	3.24	-0.57	2.70
	-0.2	-1.126	-1.167	3.64	-1.161	3.11	-1.124	-0.18	-1.12	-0.53
	-0.3	-1.879	-2.024	7.72	-1.879	0.00	-1.863	-0.85	-1.871	-0.43
				1.56		2.00		0.74		0.58
	NR70									
	-0.1	-0.773	-0.653	-15.52	-0.816	5.56	-0.826	6.86	-0.825	6.73
	-0.2	-1.491	-1.524	2.21	-1.575	5.63	-1.488	-0.20	-1.483	-0.54
	-0.3	-2.462	-2.763	12.23	-2.456	-0.24	-2.394	-2.76	-2.394	-2.76
				-0.36		3.65		1.30		1.14
	NR80									
	-0.1	-1.364	-1.217	-10.78	-1.497	9.75	-1.491	9.31	-1.45	6.30
	-0.2	-2.594	-2.91	12.18	-2.64	1.77	-2.562	-1.23	-2.658	2.47
	-0.3	-4.649	-5.425	16.69	-4.422	-4.88	-4.567	-1.76	-4.66	0.24
				6.03		2.21		2.10		3.00
Shear	NR40									
	0.1	0.058	0.041	-29.31	0.041	-29.31	0.044	-24.14	0.044	-24.14
	0.2	0.105	0.082	-21.90	0.083	-20.95	0.087	-17.14	0.087	-17.14
	0.3	0.146	0.123	-15.75	0.123	-15.75	0.129	-11.64	0.129	-11.64
				-22.32		-22.01		-17.64		-17.64
	NR50									
	0.1	0.064	0.046	-28.13	0.046	-28.13	0.048	-25.00	0.048	-25.00
	0.2	0.115	0.091	-20.87	0.091	-20.87	0.096	-16.52	0.096	-16.52
	0.3	0.162	0.136	-16.05	0.136	-16.05	0.142	-12.35	0.142	-12.35
				-21.68		-21.68		-17.96		-17.96
	NR60									
	0.1	0.113	0.081	-28.32	0.081	-28.32	0.085	-24.78	0.085	-24.78
	0.2	0.206	0.161	-21.84	0.161	-21.84	0.169	-17.96	0.169	-17.96
	0.3	0.289	0.241	-16.61	0.241	-16.61	0.251	-13.15	0.251	-13.15
				-22.26		-22.26		-18.63		-18.63
	NR70									
	0.1	0.186	0.125	-32.80	0.125	-32.80	0.13	-30.11	0.132	-29.03
	0.2	0.317	0.25	-21.14	0.25	-21.14	0.256	-19.24	0.262	-17.35
	0.3	0.43	0.374	-13.02	0.374	-13.02	0.382	-11.16	0.39	-9.30
				-22.32		-22.32		-20.17		-18.56
	NR80									
	0.1	0.297	0.199	-33.00	0.197	-33.67	0.2	-32.66	0.196	-34.01
	0.2	0.485	0.396	-18.35	0.393	-18.97	0.397	-18.14	0.392	-19.18
	0.3	0.648	0.592	-8.64	0.588	-9.26	0.588	-9.26	0.588	-9.26
				-20.00		-20.63		-20.02		-20.81
Tension	NR40									
	0.1	0.053	0.074	39.62	0.074	39.62	0.074	39.62	0.054	1.89
	0.2	0.188	0.151	-19.68	0.151	-19.68	0.151	-19.68	0.172	-8.51
	0.3	0.29	0.23	-20.69	0.23	-20.69	0.229	-21.03	0.287	-1.03
				-0.25		-0.25		-0.36		-2.55
	NR50									
	0.1	0.162	0.127	-21.60	0.168	3.70	0.152	-6.17	0.156	-3.70
	0.2	0.264	0.24	-9.09	0.275	4.17	0.27	2.27	0.273	3.41
	0.3	0.351	0.342	-2.56	0.35	-0.28	0.363	3.42	0.364	3.70
				-11.09		2.53		-0.16		1.14
	NR60									
	0.1	0.307	0.22	-28.34	0.327	6.51	0.285	-7.17	0.301	-1.95
	0.2	0.497	0.416	-16.30	0.508	2.21	0.492	-1.01	0.491	-1.21
	0.3	0.627	0.594	-5.26	0.619	-1.28	0.648	3.35	0.63	0.48
				-16.63		2.48		-1.61		-0.89
	NR70									
	0.1	0.294	0.184	-37.41	0.337	14.63	0.274	-6.80	0.291	-1.02
	0.2	0.474	0.385	-18.78	0.49	3.38	0.459	-3.16	0.485	2.32
	0.3	0.612	0.593	-3.10	0.573	-6.37	0.604	-1.31	0.633	3.43
				-19.77		3.88		-3.76		1.58
	NR80									
	0.1	0.542	0.384	-29.15	0.574	5.90	0.503	-7.20	0.541	-0.18
	0.2	0.854	0.791	-7.38	0.844	-1.17	0.868	1.64	0.869	1.76
	0.3	1.115	1.204	7.98	1.037	-7.00	1.157	3.77	1.115	0.00
				-9.52		-0.75		-0.60		0.52

Benchmark Anlaysis:

An anti-vibration part, whose mechanical responses are known, was also modeled in finite element software according to the boundary conditions of quality tests.

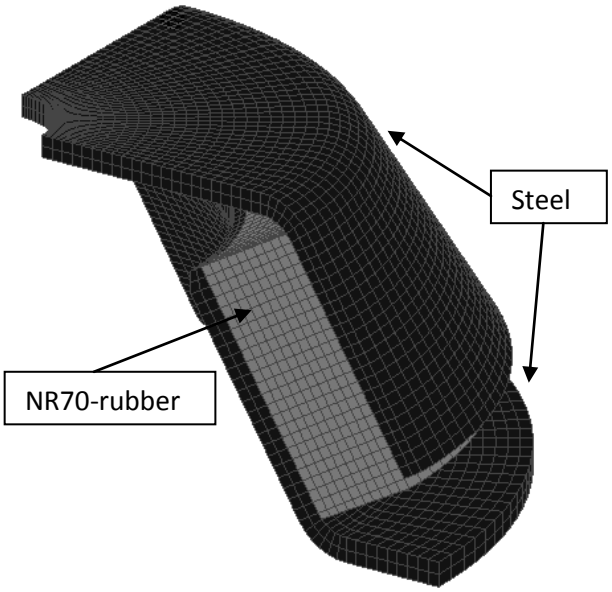

Figure 24. FEM model of anti-vibration mount

Figure 24 shows the finite element model of anti-vibration mount (AVM). Finite element model of AVM consists of 14976 8-node hexagonal elements. The nodes at the very bottom of lower metal were constrained to have no translation in all directions, while the upper steel is displaced by 4 mm during the analysis.

The material models were obtained for two different combinations of stress strain data. In other words Mooney- Rivlin and Ogden material coefficients were obtained for both tensile-simple shear and compression-shear stress-strain data. The results were shown in figures 25 and 26 with respect to real test data.

According to the Figures 25 and 26, one can say that the material models obtained from shear and compression stress-strain data give more accurate results. This can also be expected since the principal loading modes for this problem are mainly compression and shear. In order to have a numerical comparison between the material models obtained from different experimental data combinations the corresponding load values for each material model is given at the deflection 2 mm in Table 6.

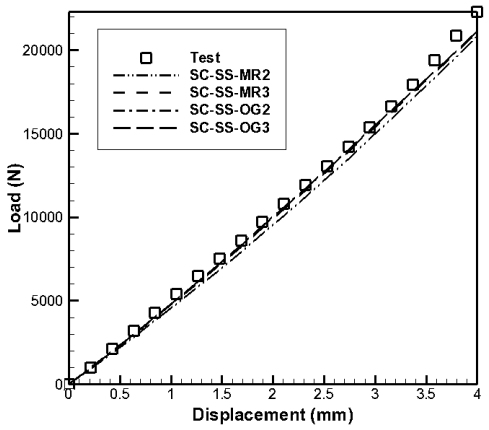

Figure 25. Comparison between FEM and real test results using compressive and simple shear stress-strain data.

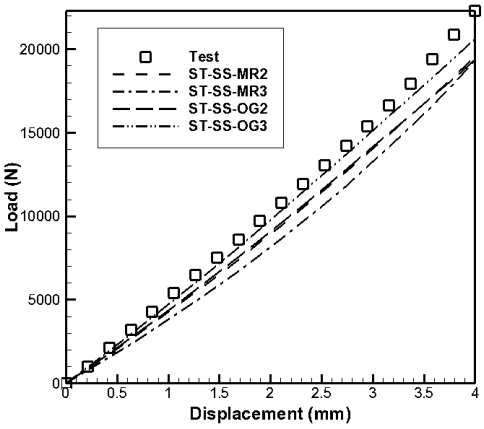

Figure 26. Comparison between FEM and real test results using tensile and simple shear stress-strain data.

Table 6. Comparison of material models for the benchmark problem(Real value: 10263.5N@ 2mm)

Material Model	Load at 2 mm (N)	Deviation (%)
SC-SS-MR2	9538.3	-7.06582
SC-SS-MR3	9904.81	-3.49481
SC-SS-OG2	10018.6	-2.38613
SC-SS-OG3	9988.87	-2.67579
ST-SS-MR2	8930.93	-12.9836
ST-SS-MR3	8155.7	-20.5369
ST-SS-OG2	9094.29	-11.3919
ST-SS-OG3	9775.19	-4.75773

5. DISCUSSIONS

According to the figures and Table 5 given in the previous section, one can conclude that all material models give better agreement in compressive loading mode. For compressive loads, the error between the real test data and material models decreases when the order of Mooney-Rivlin material model function increases. When a three coefficient Mooney Rivlin material model is selected, the accuracy of FEM solution increases compared to a two coefficient MR material model. It was found that a two coefficient material model can not account for the relation between stress and strain at relatively higher strain values. On the other hand both 2nd and 3rd order Ogden material models can fit the test data successfully. For shear loads, the best material model can be found as 2nd order Ogden material model throughout the whole strain range. Only this material model can account for the rapid increase in the stress at higher shear strain values (e.g. more than 0.75). For all material models, one can conclude that stress-strain curves obtained from material models fit the real stress strain values better as the value of shear strain value increases up to approximately 0.75. It can also obviously seen that the curves obtained from all material model functions are below the real test data. One can maybe offset the raw shear stress-strain data to make the curves fitted from the models closer to the real stress-strain values.

In the case of tensile loadings, the results were similar to the results of compressive loads. Generally, Ogden material models of both 2nd and 3rd order give better accuracy compared to Mooney Rivlin material models. One coefficient Mooney-Rivlin material model cannot account for the nonlinearities between stress and strain while a two coefficient material model can the non-linearity between stress and strain account. However, even a three coefficient Mooney-Rivlin material model cannot fit the real test data as the 2nd order Ogden material model. Figures 4 and 5 have also very interesting and important outcomes. On can see from Figure 4 that the hysteresis values obtained for compressive and shear loadings approach to each other as the value of hardness increases. It is the direct cause of percentage of carbon black amount mixed in the compound to increase the modulus. Figure 5 shows that compressive modulus much higher than both tensile and shear modulii and increases more rapidly than tensile and shear modulii as the hardness of compound increases.

6. CONCLUSION

In this study a test method using standard geometry test specimens were introduced for tensile, compressive and shear stress-strain relations, which were used to obtain the coefficients of constitutive hyper-elastic material models to be used in finite element solutions. The accuracy and precision of most widely used hyper-elastic material models (e.g. Mooney-Rivlin 2 and 3 coefficients, Ogden 2nd and 3rd order) were presented and discussed for five different natural rubber compounds having hardness values varying from 40 to 80 ShA.

An AV mount of known mechanical properties was also modeled and solved using finite element method. In order to construct the hyper-elastic material model of elastomer used for this AV mount, different combination of stress-strain data were used and out coming results were compared with the real test results. Bothe graphical and numerical comparisons were given to show the accuracy of material models.

REFERENCES

1. Peng S., Chang W., "**A Simple Approach in Finite Element Analysis of Rubber-Elastic Material",** Computer & Structures, Vol. No.3, pp. 573-593.

2. Arruda E., Boyce M., 1993, "**A Three Dimensional Constitutive Model for The Large Stretch Behavior for Rubber Elastic Materials**", J. Mech Phys. Solids, Vol. 41, No.2 PP. 389-412

3. Sasso M., Palmeieri G., Chiappini G., Amodio D., 2008, "**Characterization of hyperelastic rubber-like materials by biaxial und uniaxial stretching tests based on optical methods**" , Polymer Testing, Vol.27, pp. 995-1004.

4. Selvaduari A.P.S., 2006, "**Deflections of a rubber membrane**", Journal of Mechanics and Physics of Solids, Vol.54, pp. 1093-1119.

5. Kim J.K., Jeong O.C., Kim T.K., 2011, "**Measurement of nonlinear mechanical properties of PDMS elastomer**", Microelectronic Engineering, Vol.88, pp. 1982,1985.

6. Gent A.N, 2001, "**Engineering with rubber**", 2nd Ed., Carl Hanser Verlag, Munich.

7. Serbest A.K, Kayacı S., 2011, "**A finite element study on plastic deformation of suspension bushing**", MSC Software Users Conference 2011, İstanbul.